J|A|C|S
COMMUNICATIONS

Published on Web 02/06/2002

An Effective Method for the Discrimination of Motional Anisotropy and Chemical Exchange

Julie M. Kneller, Min Lu, and Clay Bracken*

Department of Biochemistry, Weill Medical College of Cornell University, New York, New York 10021

Received November 2, 2001

Heteronuclear spin-relaxation rates have proven to be powerful probes of the overall and internal dynamics of macromolecules.[1,2] Accurate assessment and interpretation of spin-relaxation data requires careful consideration of anisotropic rotational diffusion and chemical exchange.[3−10] A commonly used approach for the analysis of heteronuclear relaxation data examines the ratio between transverse and longitudinal rates, R_2/R_1, for identification of residues undergoing chemical exchange and estimation of global correlation times.[11] The R_2/R_1 approach does not distinguish between the effects of motional anisotropy and chemical exchange. This communication describes a method for separating the effects of chemical exchange from motional anisotropy by analysis of the product of R_1R_2. The results demonstrate that the R_1R_2 analysis significantly attenuates the effects of motional anisotropy. Furthermore, the method permits rapid identification of chemical exchange, R_{ex}, and direct estimation of the order parameters, S^2. The utility of R_1R_2 analysis is shown by using two proteins: *E. coli* ribonuclease H (RNaseH)[12,13] and the *E. coli* trimeric coiled-coil outer membrane lipoprotein (Lpp51).[14]

In well-structured regions of proteins, the majority of backbone motions can often be modeled by using the simplest form of the Lipari−Szabo model-free spectral density function, $J(\omega)$.[15] Model-free function assumes that spectral density is dominated solely by correlation time, τ_c, which is scaled by subpicosecond motions represented by S^2. The simplified spectral density equation is:

$$J(\omega) = \frac{S^2\tau_c}{(1 + \omega^2{\tau_c}^2)} \qquad (1)$$

where ω is the Larmor frequency. When $\omega\tau_c \gg 1$, the R_1 and R_2 relaxation rates are dominated by contributions from spectral densities $J(\omega_X)$ and $J(0)$, respectively. In proteins, ω_X is generally the Larmor frequency for ^{13}C or ^{15}N heteronuclei for which relaxation rates are monitored. For instance, for backbone ^{15}N relaxation rates at a field strength of 14 T, $S^2 = 0.87$, and $\tau_c = 10$ ns, over 95% of R_2 is due to $J(0)$ and 98% of R_1 is dominated by $J(\omega_N)$. The presence of R_{ex} primarily elevates the R_2 rates. The H−X bond orientation within an anisotropic molecule influences the local correlation time experienced by the nuclei, resulting in divergence between the R_1 and R_2 rates. Analysis with R_2/R_1 obscures the distinction between effects of chemical exchange and anisotropic motion. This difficulty can be circumvented by consideration of the product R_1R_2 when $\omega\tau_c \gg 1$ where

$$R_1R_2 \propto J(0)J(\omega_x) \cong \frac{S^4}{{\omega_x}^2} \qquad (2)$$

In the absence of internal motion, when $S^2 = 1$, R_1R_2 is essentially constant at a given magnetic field, provided $\omega_x\tau_c \gg 1$. The R_1R_2 values are exquisitely sensitive to the presence of fast motions that reduce the R_1R_2 product. The presence of slower μs−ms motional processes associated with R_{ex} increases R_1R_2 values. Variations in R_1R_2 due to motional anisotropy are nullified as τ_c is now absent.

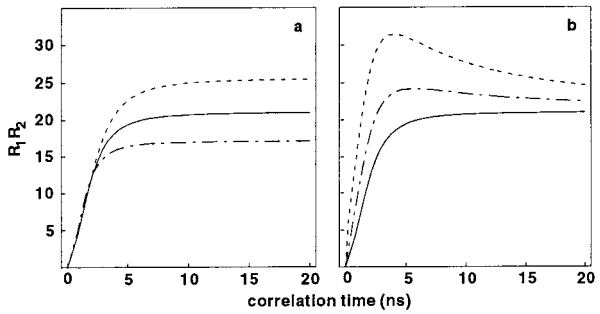

Figure 1. The product of R_1R_2 is plotted as (a) a function of the rotational correlation time τ_c and magnetic field strengths 11.7 (dashed), 14.0 (solid), and 18.7 T (dot−dashed). (b) Values of R_1R_2 are plotted at 14.0 T in the presence of R_{ex} values of 0 (solid), 2.0 (dot−dashed), and 5.0 s^{-1} (dashed). The R_1 and R_2 rates were calculated for the ^{15}N backbone nuclei by using the spectral density function given in eq 1, with variables $S^2 = 1$, an ^{15}N chemical shift anisotropy value of $\Delta\sigma = -172$, and a $^1H-^{15}N$ bond distance of $r_{HN} = 1.02$ Å.

Theoretical curves of R_1R_2 plotted as a function of τ_c at magnetic field strengths 11.7, 14, and 18.7 T are shown in Figure 1a. As $\omega_x\tau_c$ increases, the product R_1R_2 approaches a constant value. Higher B_0 field strengths better fulfill the condition $\omega_x\tau_c \gg 1$ thereby extending the plateau of constant R_1R_2 values to a greater range of correlation times. The effects of chemical exchange significantly raise R_1R_2, as shown in Figure 1b. Increases in $\Delta\sigma$ or reductions in r_{HX} values result in an upward shift of curves shown in Figure 1.

The upper limit of the R_1R_2 values, when $R_{ex} = 0$ and $S^2 = 1$, allows direct estimation of the average generalized order parameters ${S_{av}}^2$ from experimentally observed R_1R_2 values as shown:

$${S_{av}}^2 = \sqrt{\langle R_1R_2\rangle / {R_1R_2}^{max}} \qquad (3)$$

where ${R_1R_2}^{max}$ is the calculated maximum value and $\langle R_1R_2\rangle$ is the experimentally observed 10% trimmed mean value after exclusion of residues with low NOE values. Similarly, estimates of the chemical exchange rates can be obtained by examining residues that significantly deviate above $\langle R_1R_2\rangle$.

The *E. coli* protein RNaseH serves to demonstrate this method because both chemical exchange and significant anisotropic motions are present.[12,13] Anisotropic effects are easily observed in the relaxation rates of helix D where residues V101 and L111 have HN bond vectors aligned with the long axis of the diffusion tensor.[16] Direct measurement of chemical exchange in RNaseH has revealed that two resonances, K60 and W90, have rates in excess of 1 s^{-1}.[16] A plot of R_2/R_1 values for RNaseH is shown in Figure 2a. It is not readily apparent which residues are outliers due to exchange and

10.1021/ja017461k CCC: $22.00

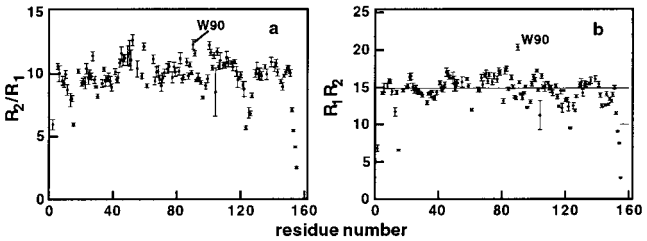

Figure 2. ^{15}N relaxation data for 17.6 kD U−^{15}N labeled *E. coli* RNaseH at pH 5.5, 300 K, 0.8 mM, and 14 T field strength.[1] (a) The R_2/R_1 ratio and (b) the R_1R_2 product are plotted as a function of amino acid sequence. Residue W90 displays chemical exchange. The residue K60 is not included due to extreme chemical exchange broadening which places it off-scale in both panels. The line at $R_1R_2 = 14.9$ indicates the $\langle R_1R_2 \rangle$ mean value corresponding to $S^2 = 0.86$.

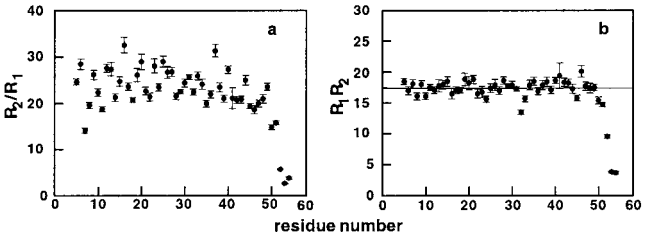

Figure 3. ^{15}N relaxation data for 16 kD U−^{15}N labeled *E. coli* periplasmic lipoprotein Lpp51 at pH 5.8, 308 K, and 1.0 mM at 14 T field strength. (a) R_2/R_1 and (b) R_1R_2 are plotted as a function of amino acid sequence. Significant variations due to the high degree of molecular anisotropy are evident in the R_2/R_1 plot. Anisotropic variations largely cancel in the R_1R_2 presentation. This indicates that variations in the R_2/R_1 plot are predominantly due to rotational anisotropy. The line at $R_1R_2 = 17.4$ indicates the $\langle R_1R_2 \rangle$ mean value corresponding to $S^2 = 0.92$. Heteronuclear relaxation data were acquired and processed using procedures described previously.[17]

fast motional processes. In contrast, R_1R_2 plots reduce deviations due to anisotropic motion revealing W90 as a significant outlier. The variations in the R_1R_2 values diminish with increasing field strength since the condition $\omega_x\tau_c \gg 1$ is more fully satisfied.

The values of $\langle R_1R_2 \rangle$ were calculated for magnetic field strengths of 11.7, 14, and 18.7 T after excluding residues with NOE values <0.65 at field strengths of 11.7 and 14 T and NOE values <0.7 at 18.7 T. On the basis of deviation from the R_1R_2 mean, the estimated R_{ex} values for W90 were 2.8 ± 1.8, 4.2 ± 1.6, and 6.9 ± 1.3 s^{-1} at field strengths 11.7, 14, and 18.7 T, respectively. Estimated order parameters determined from mean R_1R_2 values of RNaseH, at magnetic field strengths of 11.7, 14, and 18.7 T were 0.84 ± 0.08, 0.86 ± 0.04, and 0.88 ± 0.05, respectively. The measured $\Delta\sigma$ values display site-to-site variations of 5.5 ppm in RNaseH[13] resulting in 3−4% variability in R_1R_2 values. Changes in both S^2 and $\Delta\sigma$ values may potentially mask small chemical exchange rates. However, the R_1R_2 estimated values for S^2 and R_{ex} are in good agreement with prior measurements in RnaseH, where $S^2 = 0.854 \pm 0.002$ and W90 displays an exchange rate of 2.46 ± 0.53 s^{-1} at 11.7 T.[12,13,16]

^{15}N relaxation data on the Lpp51 coiled-coil trimer provide an example of extreme motional anisotropy.[14] Analysis of the crystal structure indicates that the angle between the HN bond vectors of the α-helices and the trimer symmetry axis varies between 0° to 45° in the coiled-coil. Calculation of the diffusion anisotropy for Lpp51 with HYDRONMR[18] estimates the ratio of the perpendicular to the parallel axial diffusion tensor $D_\parallel/D_\perp = 3.75$. Due to the high degree of anisotropy, significant variations in the R_2/R_1 values are observed (Figure 3a). In contrast, the R_1R_2 product significantly reduces scatter due to anisotropic motions. Direct measurement of chemical exchange effects in Lpp51 with use of the relaxation compensated CPMG sequence[8] indicates that no chemical exchange rates in excess of 2 s^{-1} are present. Overall S^2 values for Lpp51 are estimated to be 0.92 ± 0.08, a value similar to the higher order parameters observed in the coiled-coil region of GCN4, $S^2 = 0.91 \pm 0.03$.[17]

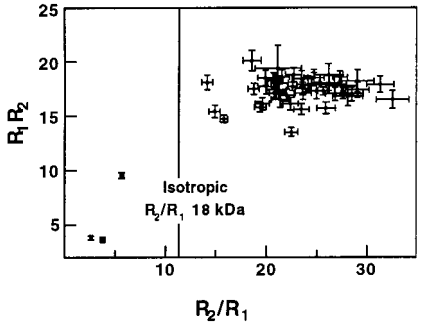

Figure 4. ^{15}N relaxation data for Lpp51 are displayed as R_1R_2 vs R_2/R_1. The line displays the calculated R_2/R_1 value for an 18 kDa isotropic protein. The distribution of ^{15}N relaxation rates indicates a strong bias in the orientation of the HN bond vectors and a highly anisotropic structure.

We have presented a rapid method for estimating and dissociating the effects of motional anisotropy and chemical exchange in spin relaxation data. The simplicity of the method will allow better initial estimates of the relaxation parameters for use in more detailed dynamics analyses. The R_1R_2 analysis method clarifies the interpretation of R_2/R_1 ratios by providing criteria for exclusion of data that displays chemical exchange and fast motional effects. By eliminating significant sources of error, this method improves upon the use of R_2/R_1 ratios in NMR structural analysis.

Acknowledgment. We thank C. D. Kroenke, J. P. Loria, J. A. Butterwick, A. G. Palmer III, and M. Rance for NMR relaxation data collected on *E. coli* RNaseH. We thank A. G. Palmer III and L. G. Werbelow for careful reading of the manuscript. This work was supported by a Charles H. Revson Fellowship (J.M.K.), by the American Heart Association (C.B.), and by a Stanley Stahl Fellow (C.B.).

Supporting Information Available: Graphs of R_2/R_1 and R_1R_2 vs amino acid sequence for RNaseH at 11.7, 14, and 18.8 T; plots showing R_1R_2 vs R_2/R_1 for RNaseH; detailed derivation of the R_1R_2 relation (PDF). This material is available free of charge via the Internet at http://pubs.acs.org.

References

(1) Kay, L. E. *Nat. Struct. Biol.* **1998**, *NMR Suppl.*, 513−517.
(2) Palmer, A. G. *Annu. Rev. Biophys. Biomol. Struct.* **2001**, *30*, 129−155.
(3) Woessner, D. E. *J. Chem. Phys.* **1962**, *36*, 1−4.
(4) Schurr, J. M.; Babcock, H. P.; Fujimoto, B. S. *J. Magn. Reson. B* **1994**, *105*, 211−224.
(5) Akke, M.; Palmer, A. G. *J. Am. Chem. Soc.* **1996**, *118*, 911−912.
(6) Phan, I. Q. H.; Boyd, J.; Campbell, I. D. *J. Biomol. NMR* **1996**, *8*, 369−378.
(7) Lee, L. K.; Rance, M.; Chazin, W. J.; Palmer, A. G. *J. Biomol NMR* **1997**, *9*, 287−298.
(8) Loria, J. P.; Rance, M.; Palmer, A. G. *J. Am. Chem. Soc.* **1999**, *121*, 2331−2332.
(9) de Alba, E.; Babar, J. L.; Tjandra, N. *J. Am. Chem. Soc.* **1999**, *121*, 4282−4283.
(10) Pawley, N. H.; Wang, C.; Koide, S.; Nicholson, L. K. *J. Biomol. NMR* **2001**, *20*, 149−165.
(11) Kay, L. E.; Torchia, D. A.; Bax, A. *Biochemistry* **1989**, *28*, 8972−8979.
(12) Mandel, A. M.; Akke, M.; Palmer, A. G. *J. Mol. Biol.* **1995**, *246*, 144−163.
(13) Kroenke, C. D.; Rance, M.; Palmer, A. G. *J. Am. Chem. Soc.* **1999**, *121*, 10119−10125.
(14) Shu, W.; Liu, J.; Ji, H.; Lu, M. *J. Mol. Biol.* **2000**, *299*, 1101−1112.
(15) Lipari, G.; Szabo, A. *J. Am. Chem. Soc.* **1982**, *104*, 4546−4559.
(16) Kroenke, C. D.; Loria, J. P.; Lee, L. K.; Rance, M.; Palmer, A. G. *J. Am. Chem. Soc.* **1998**, *120*, 7905−7915.
(17) Bracken, C.; Carr, P. A.; Cavanagh, J.; Palmer, A. G. *J. Mol. Biol.* **1999**, *285*, 2133−2146.
(18) de la Torre, J. G.; Huertas, M. L.; Carrasco, H. B. *J. Magn. Reson.* **2000**, *147*, 138−146.

JA017461K